Determination of Surface Fluxes from the Surface Radiative Temperature

JIELUN SUN AND L. MAHRT

College of Oceanic and Atmospheric Sciences, Oregon State University, Corvallis, Oregon

(Manuscript received 27 June 1994, in final form 26 August 1994)

ABSTRACT

This study examines the bulk aerodynamic method for estimating surface fluxes of heat and moisture using the surface radiative temperature. The surface radiative temperature is often the only available surface temperature from field measurements. Models typically predict heat fluxes from the surface radiative temperature computed from the surface energy balance. In this study, the corresponding *radiometric exchange coefficient* and *radiometric roughness height* are computed from tower- and low-level aircraft data taken during four different field programs. The data analysis shows that the radiometric exchange coefficient does not increase with increasing instability. This is because the radiometric exchange coefficient must compensate for the large vertical temperature difference resulting from use of the surface radiative temperature.

The data analysis and scaling arguments indicate that the radiometric exchange coefficient for heat in the bulk aerodynamic formulation is closely related to $\theta_*/\Delta\theta$ for both stable and unstable conditions, where $\Delta\theta$ is the difference between the surface radiative temperature and the air temperature and θ_* is the negative of the heat flux divided by the surface friction velocity. Application of Monin–Obukhov similarity theory with surface radiative temperature also reduces to a relatively circular internal relationship between the *radiometric roughness height* and $\theta_*/\Delta\theta$. This roughness height is flow dependent and not systematically related to the roughness height for momentum.

As an additional complication, the observed radiometric exchange coefficient for heat depends on the relationship between the measured surface radiative temperature and the microscale distribution of surface radiative temperature in the footprint of the heat flux measurement. Analogous problems affect the prediction of the moisture flux based on the saturation vapor pressure at the surface radiative temperature.

1. Introduction

The traditional bulk aerodynamic formulation estimates the surface heat flux in terms of the difference between the potential temperature at a reference height within the surface layer and the air temperature at the roughness height for heat (aerodynamic surface temperature). The exchange coefficient for the traditional bulk aerodynamic formulation is usually related to similarity theory based on the Obukhov length or surface-layer Richardson number. The air temperature at the roughness height cannot be directly measured but can be inferred by extrapolating a similarity prediction of the temperature profile to the roughness height for momentum. For this reason, the temperature at the roughness height is often replaced by the surface radiative temperature, which is more easily measured. This replacement is particularly useful in numerical models of the boundary layer that relate the heat and moisture fluxes to a surface radiative temperature computed from the surface energy budget. Unfortunately, with surface heating or cooling, the surface radiative temperature may be significantly different from the aerodynamic temperature at the roughness height leading to errors in the existing similarity prediction of the heat and moisture fluxes.

Choudhury et al. (1986), Beljaars and Holtslag (1991), and Hall et al. (1992) found that the surface radiative temperature is 2–6°C higher than the inferred aerodynamic temperature under unstable atmospheric conditions and lower than the aerodynamic temperature under stable conditions. Therefore, for unstable conditions, the difference between the surface aerodynamic temperature at the roughness height and the air temperature at the observational height within the surface layer is overpredicted by use of the surface radiative temperature. Then the bulk aerodynamic formula using traditional similarity theory and the surface radiative temperature overestimates the actual heat flux, particularly over bare ground or ground covered with only sparse vegetation. As a result, a "radiometric exchange coefficient" must be specified for use of surface radiative temperature whose value is significantly smaller than that predicted by existing similarity theory. Equivalently, Kustas et al. (1989) and Kohsiek et al. (1993) found that when the surface radiative temperature is used, the radiometric resistance for heat is

Corresponding author address: Dr. L. Mahrt, College of Oceanic and Atmospheric Sciences, Oregon State University, Corvallis, OR 97331-2209.

higher than the traditional resistance for similarity theory. Over a full canopy cover with unstressed transpiration, the surface radiative temperature is closer to the surface aerodynamic temperature leading to smaller errors in heat flux predicted by traditional similarity theory.

There are four existing ways to reduce the error caused by replacement of the aerodynamic surface temperature with the surface radiative temperature.

Approach 1: Determine a new stability function for the radiometric exchange coefficient that predicts the correct heat flux when the surface radiative temperature is used (Brutsaert 1992).

Approach 2: Replace the roughness height with the "radiometric roughness height" defined to be the roughness height adjusted so that use of the surface radiative temperature in the usual similarity formulation correctly predicts the heat flux (Kustas et al. 1989; Sugita and Brutsaert 1990; Kohsiek et al. 1993).

Approach 3: Formulate an empirical formula between the surface aerodynamic temperature and the surface radiative temperature (Zilitinkevich 1970; Garratt and Francey 1978; Brutsaert 1982). Such a relationship can be posed in terms of the roughness height for heat. This roughness height can be inferred from either an assumed relationship between roughness heights for momentum and heat or from the assumed relationship between vegetation height and roughness height for heat (Choudhury et al. 1986; Brutsaert 1982).

Approach 4: Retain the traditional roughness height for heat and introduce an extra resistance term due to the difference between the temperature at roughness height and surface radiative temperature. Lhomme et al. (1988) found that replacing the aerodynamic temperature with the surface radiative temperature is equivalent to introducing an extra resistance term. The new resistance term in Lhomme et al. (1988) was derived for full canopy cover and depended on canopy structure and wind velocity.

This study examines approaches 1 and 2 in sections 3 and 4, respectively. Radiometric roughness heights derived from different stability functions are compared in section 5.

2. Data

This study analyzes six aircraft and two tower datasets. The aircraft data includes eight runs over the same track on each of two fair weather days during the California Ozone Deposition Experiment (CODE) (Table 1). Spatial variations of the flux along this track are described in Sun and Mahrt (1994). This study also analyzes data from two tower sites in CODE, one in a large cotton field several kilometers across (Delany et al. 1993) and one in a large vineyard about 1 km across located within a region of predominantly grape vineyards (den Hartog et al. 1992). The data for the two sites are described in Pederson et al. (1994). The cotton site is located 80 km west of Fresno in the San Joaquin Valley of California on flat terrain with few obstructions. Surface radiation temperature at the cotton site was measured with an Everest Interscience radiometer 4 m above the ground surface. The fluxes were computed using a 3D sonic anemometer from the University of Washington, a fast-response temperature sensor from Atmospheric Instrumentation Research, and a fast-response humidity from a Campbell Scientific Krypton hygrometer. The fluxes were computed from 30-min averages (Delany et al. 1993). The vineyard site (Thompson seedless green grapes) was located over flat terrain near Madera, California. The surface radiative temperature of the vegetation was measured with a Barnes PRT-5 radiometer, while the surface temperature of the soil was measured with an InterScience 4000A infrared thermometer, calibrated relative to the Barnes PRT-5 radiometer. Fluxes were computed using a Kaijo Denki 3D sonic anemometer and an AIR hygrometer LA-1 and averaged over 30-min periods (den Hartog et al. 1992).

TABLE 1. Data.

Field program	Observation level (m)	References
ASTER Tower, cotton site	5	Delany et al. 1993
AES Tower, vineyard site	10	den Hartog et al. 1992
BLX83	60–120	Stull 1994
CODE Flight 13	30	MacPherson 1992
CODE Flight 19	30	MacPherson 1992
HAPEX, 19 May 1986	125	Mahrt 1991
HAPEX, 25 May 1986	125	Mahrt 1991
buFex, Lake King	12	Lyons et al. 1993

Additional aircraft data are analyzed from the Boundary Layer Experiment-1983 (BLX83) near Chickasha, Oklahoma (Stull 1994), from the Bunny Fence Experiment (buFex) in the Lakes District of the Great Southern Region of Western Australia (Lyons et al. 1993), and from the Hydrological and Atmospheric Pilot Experiment (HAPEX) in Southwest France. The aircraft data in HAPEX and some of the aircraft data in BLX were taken at about 125 m above ground, well above the traditional top of the surface layer (~30 m). These datasets appear to obey the same similarity theory as data taken within the surface layer. This agreement may be due to the fact that the potential temperature θ was well mixed above the surface, and the heat flux probably decreased by only about 10% between the surface and 125 m.

For the aircraft data from CODE, HAPEX, and buFex, mean values of the variables are computed as an unweighted average over a 5-km moving window. To compute the fluxes, products of perturbations from these averages are computed and averaged over the same 5-km moving window. The fluxes from BLX83

are averaged over the entire flight leg of 20 km as reported in Stull (1994).

3. Radiometric exchange coefficient for heat flux

a. Traditional similarity theory

The traditional bulk aerodynamic formula for heat can be expressed as

$$\overline{w'\theta'} = C_h U[\theta_{z_h} - \theta(z)], \tag{1}$$

where θ_{z_h} and $\theta(z)$ are the potential temperatures at the roughness height for heat and at the observational height, respectively. Here U is the mean wind speed at the observational height, and C_h is the exchange coefficient.

The exchange coefficient for heat based on the traditional Monin–Obukhov similarity theory can be formulated as

$$C_h = \frac{k^2}{[\ln(z/z_m) - \Psi_m(z/L)][\ln(z/z_h) - \Psi_h(z/L)]}, \tag{2}$$

where Ψ_m and Ψ_h are the stability functions for momentum and heat, respectively, k is the von Kármán constant, z is the observational height within the surface layer, z_m and z_m are the roughness heights for momentum and heat, respectively, and L is the Obukhov length. Based on Paulson (1970), the stability functions can be expressed as

$$\Psi_m(z/L) = \begin{cases} -5z/L & 0 < z/L < 1 \\ 2\ln[(1+x)/2] + \ln[(1+x^2)/2] & \\ \quad - 2\tan^{-1}(x) + \pi/2 & -5 < z/L < 0 \end{cases}$$

$$\Psi_h(z/L) = \begin{cases} -5z/L & 0 < z/L < 1 \\ 2\ln[(1+x^2)/2] & -5 < z/L < 0, \end{cases}$$

where

$$L = -\overline{\theta_v} u_*^3/(kg\overline{w'\theta_v'})$$

$$x = (1 - 16z/L)^{1/4}.$$

Here θ_v is the virtual potential temperature, u_* is the friction velocity, and g is the acceleration of gravity. The displacement heights are small compared to the observational levels and are omitted in this study for simplicity.

b. Radiometric exchange coefficient

According to (2), the exchange coefficient should increase with increasing instability, given roughness heights for momentum and heat. However, this stability dependence cannot be extended to the *radiometric exchange coefficient* for heat C_{hr}, which is defined in the bulk aerodynamic relationship of the form

$$\overline{w'\theta'} = C_{hr} U \Delta\theta, \tag{3}$$

where

$$\Delta\theta = \theta_{\text{sfc}} - \theta(z).$$

Here θ_{sfc} is the potential temperature corresponding to the surface radiative temperature. The traditional exchange coefficient in (2) increases with increasing instability (negative z/L) as shown in Fig. 1 by evaluating (2) for $z = 10$ m, $z_m = 0.01$ m, $z_h = 0.01$ m, and 10^{-4} m. However, considering the large scatter in Fig. 1, any dependence of the radiometric exchange coefficient on stability is weak. Scatter is particularly large in the near neutral regime (large Obukhov length) corresponding to weak upward heat flux. This regime includes numerous negative values of C_{hr} corresponding to upward heat flux and negative values of $\Delta\theta$. These countergradient cases occur only in the tower observations of fluxes over irrigated crops, as is evident in Fig. 2 where the tower and aircraft data are plotted separately. Figure 2 defines three stability regimes: the unstable regime corresponding to upward gradient heat flux (positive $-\theta_*$ and $\Delta\theta$ in Fig. 2), the stable regime corresponding to downward gradient transport of heat (negative $-\theta_*$ and $\Delta\theta$ in Fig. 2), and the countergradient regime corresponding to weak upward heat flux ($-\theta_*$ and $\Delta\theta$ have opposite signs). The temperature scale θ_* is defined as $-\overline{w'\theta'}/u_*$. The special countergradient regime is associated with the microscale distribution of the surface radiative temperature over the irrigated crops, as will be discussed below.

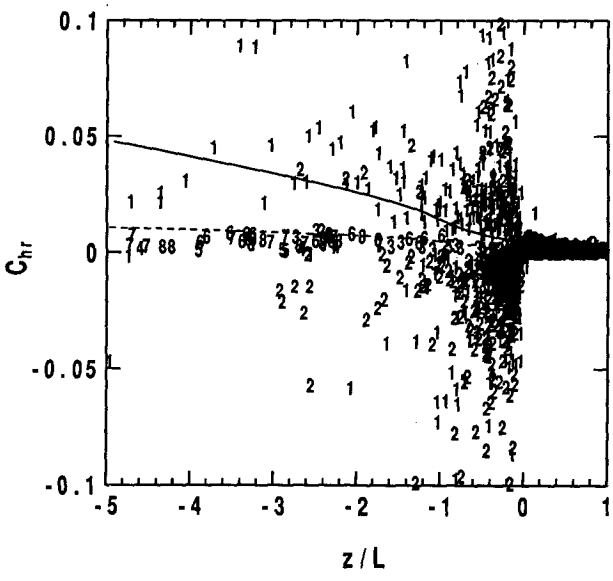

FIG. 1. C_{hr} versus z/L for all datasets collected within the stability range $-5 < z/L < 1$. Numbers represent datasets in Table 1 in sequential order. The two curves are derived from the Monin–Obukhov similarity theory [Eq. (2)] with $z = 10$ m, $z_m = 0.01$ m, $z_h = 0.01$ m (solid), and $z_h = 1 \times 10^{-4}$ m (dashed).

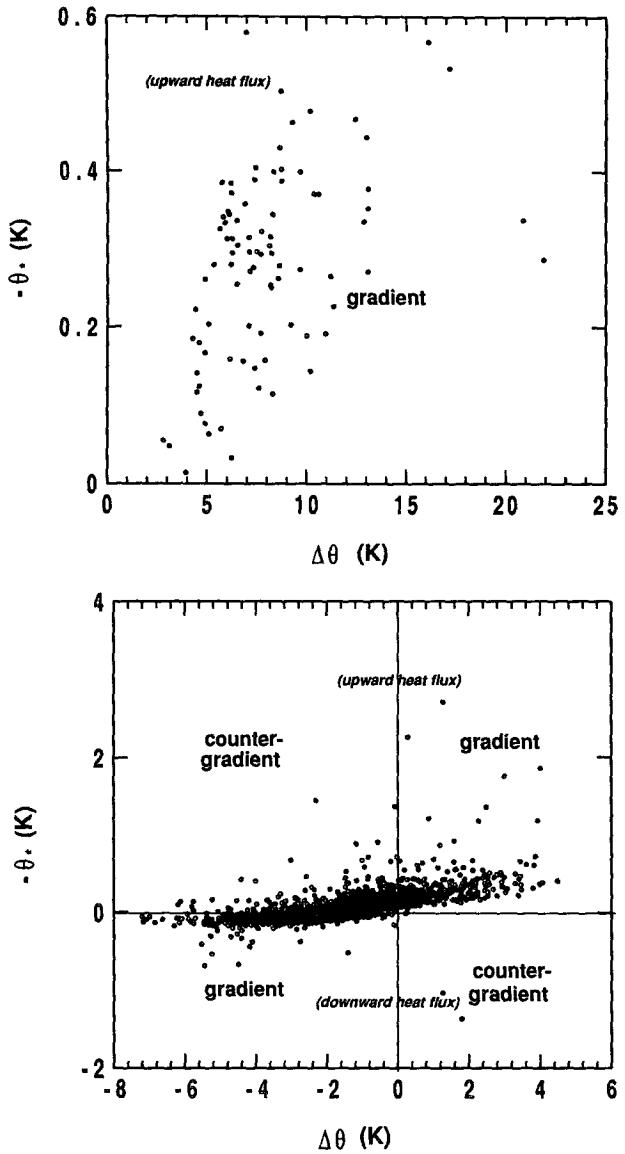

FIG. 2. (a) Aircraft data and (b) tower data plotted in phase space based on $-\theta_*$ and $\Delta\theta$.

The difference of the stability dependence between the usual exchange coefficient and the radiometric exchange coefficient in Fig. 1 is partly due to the observed more rapid increase of $\Delta\theta$ with increasing instability (large negative z/L) compared to the increase of $\theta_{z_h} - \theta(z)$ with increasing instability. That is, for large instability, the use of surface radiative temperature leads to a larger vertical temperature difference, which requires a smaller exchange coefficient in order to predict the correct heat flux. This behavior of the radiometric exchange coefficient suggests that the usual stability function for similarity theory must be significantly altered or that the radiometric roughness height at a given location is not constant. The latter will be discussed in the next section.

Attempts to modify the stability function for existing similarity theory fail for the present datasets because z/L does not adequately account for the variability of the radiometric exchange coefficient. As a result, the near stability independence of C_{hr} for unstable conditions ($z/L < 0$) cannot be included by simply adjusting the constant value of the roughness height for heat in existing similarity theory (Fig. 1). The behavior of the radiometric exchange coefficient can be explored by rewriting the bulk aerodynamic relationship as

$$C_{hr} = \overline{w'\theta'}/(\Delta\theta U) \equiv -\theta_* u_*/(\Delta\theta U). \quad (4)$$

For the present datasets, u_*/U varies much more slowly than $\theta_*/\Delta\theta$ when the vertical temperature difference is expressed in terms of the surface radiative temperature. The larger variation of $\theta_*/\Delta\theta$ is due to large variation of the surface radiative temperature. In fact, Fig. 3 suggests that a simple relation of the form

$$C_{hr} = a(-\theta_*/\Delta\theta) \quad (5)$$

can explain most of the variation of C_{hr}. The constant coefficient a is now evaluated after excluding extreme values of the exchange coefficient. Such large values are associated with significant heat flux and near zero temperature difference, in which case small errors in the temperature measurements lead to large errors in the exchange coefficient. Arbitrarily, the largest 10% of the extreme values of the exchange coefficient have been excluded in Fig. 3 and the following linear regression analysis. The nonzero constant in the linear regression analysis leading to (5) is extremely small and has been neglected. For these data, the best-fit

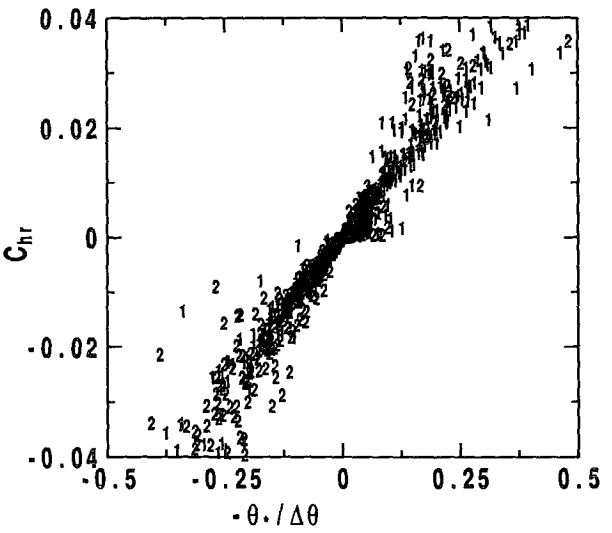

FIG. 3. The radiometric exchange coefficient C_{hr} as a function of $-\theta_*/\Delta\theta$. Numbers represent datasets in Table 1 in sequential order. Here 10% of the points are offscale.

value of the remaining coefficient is $a = 0.11$. Relationship (5) explains 96% of the variance of C_{hr}. When all of the data are used, the variance explained remains approximately the same and the coefficient changes slightly to $a = 0.10$.

Because the variation of u_*/U becomes unimportant in (4) with use of the surface radiative temperature, the data leads to a somewhat circular relationship (5), as often occurs with similarity relationships. That is, the exchange coefficient for heat depends on the heat flux itself. Consequently, the radiometric exchange coefficient, as approximated by (5), has questionable utility as a predictive scheme, but instead expresses an internal relationship between variables. Notice that $-\theta_*/\Delta\theta$ is positive for both stable and unstable cases (gradient transfer) and negative for the countergradient regimes defined in Fig. 2. Therefore, the dependence of C_{hr} on $-\theta_*/\Delta\theta$ for gradient-transfer stable cases is folded over on the top of the gradient-transfer unstable cases in Fig. 3.

Since (5) is dominated by tower data, the regression analysis was independently applied to the aircraft data alone, yielding $a = 0.12$, as opposed to $a = 0.11$ for the combined dataset. The regression relationship for the aircraft data explains 67% of the variance. The difference between the aircraft data and the total dataset are partly related to differences between spatial averages over heterogeneous surfaces (aircraft data) and local time averages over relatively homogeneous terrain (tower data). Subsequent analyses will be applied only to the combined dataset.

The excellent fit of (5) to the data implies that the heat flux can be expressed independently of the roughness height for heat when surface radiative temperature is used. The roughness of the surface influences u_* but exerts only a secondary influence on the radiometric exchange coefficient. This influence can be expressed in term of the drag coefficient C_D by writing (4) in the form

$$C_{hr} = -C_D^{1/2}\frac{\theta_*}{\Delta\theta}. \tag{6}$$

The appearance of the one-half power of C_D is due to its definition in terms of the square of U, while C_h is defined with respect to the first power of U. Relationship (6) corresponds to $a = C_D^{1/2}$ in (5). Since the coefficient in (5) is constant, deviations from (5) are generated by variations of the drag coefficient. For the data analyzed here, these deviations are minimal compared to variations of $\theta_*/\Delta\theta$.

The temperature difference $\Delta\theta$ increases with observational height, which requires the radiometric exchange coefficient to decrease with observational height in order to predict the same heat flux. However, Fig. 3 shows that the effect of the different observational heights of the various datasets are accommodated by the single curve in Fig. 3. If the reference level is moved closer to the surface, the decreasing vertical temperature difference implies more neutral conditions analogous to the role of z in the stability parameter z/L. However, this height dependence simply corresponds to moving along the single curve in Fig. 3. This height dependence partly explains the much larger exchange coefficients computed from the tower data ($z = 5$ m and 10 m) compared to those for the aircraft data ($z \geq 12$ m).

The single curve in Fig. 3 also implicitly includes the effect of variable vegetation cover. The top of the canopy represents more ventilated surfaces as opposed to bare-ground surfaces. More specifically, a leaf surface loses heat through conduction on both the upper and lower leaf surfaces. Also, compared to the ground surface, stronger wind fluctuations more efficiently sweep away heat accumulated near the leaf surfaces at the canopy top. This leads to smaller differences between the leaf radiative temperature and the aerodynamic temperature even without transpiration. However, in the formulation for the radiometric exchange coefficient (5), the effect of variable vegetation cover is implicitly included through the variation of $\Delta\theta$.

c. *Countergradient heat flux*

The different datasets contain different degrees of spatial averaging, both in terms of field of view of the tower radiometer and in terms of more extensive averaging of the aircraft-measured surface radiative temperature. The problem of averaging may be important even on the microscale. Stull (1994, his Fig. 11) shows an example of significant microscale variability of surface radiative temperature around a tower. The meaning of the surface radiative temperature becomes complicated with partial vegetation cover. The soil and vegetation may contribute to the heat flux in different proportions than their contributions to the surface radiative temperature. The complex relationship between the surface radiative temperature and distribution of vegetation is illustrated in Otterman et al. (1992). Hatfield et al. (1984) found that compositing the vegetation and soil surface temperatures leads to improved prediction of the evapotranspiration compared to use of vegetation temperatures alone.

Upward heat flux sometimes occurs with negative temperature differences (negative $\Delta\theta$), corresponding to negative values of the radiometric exchange coefficient (countergradient fluxes). Although flux-sampling problems may be significant, this behavior is apparently due mainly to the domination of the heat flux by the warmest part of the surface. For example, at the vineyard site at midday, the averaged surface radiative temperature may be slightly cooler than the air temperature, yet the heat flux is dominated by unshaded bare soil between the rows where the surface temperature is warmer than the air temperature. The present analysis of the vineyard data is based on the surface

radiative temperature of the vegetation. Use of the warmer soil radiative temperature at the vineyard site reduced the number of cases of countergradient heat flux, although a significant number of countergradient cases remain. This is because the soil radiative temperature includes some shaded soil, as well as horizontal variation of soil moisture.

The radiometric exchange coefficient is closely related to $\theta_*/\Delta\theta$ for the countergradient regime, in which case (5) remains a good approximation. However, some investigators may be uncomfortable with the negative values of the exchange coefficient. It is possible to formulate a correction to the temperature difference to eliminate negative values of the exchange coefficient. This is the subject of future investigation after more complete measurements of the microscale distribution of the surface radiative temperature are obtained.

At the transitions between the gradient and countergradient regimes, the exchange coefficient assumes extreme values. At one transition the vertical temperature difference vanishes but the heat flux remains (weak) upward. Tower data points near this transition lead to the very large values (exceeding unity in Fig. 3) of the radiometric exchange coefficient. At the second transition, the heat flux vanishes, but the temperature difference is nonzero negative. Data points near this transition correspond to extremely small values of the exchange coefficient.

4. Radiometric roughness height for heat

Since the radiometric exchange coefficient for large positive $\Delta\theta$ must be significantly smaller than that predicted by traditional similarity theory, the corresponding radiometric roughness height must be much smaller than the traditional value for heat (Beljaars and Holtslag 1991; Mahrt and Ek 1993). In fact, the radiometric roughness height may be as small as 10^{-10} m (Sugita and Brutsaert 1990; Brutsaert and Sugita 1992). In other words, the existing similarity theory can predict the correct heat flux only if unphysically small values of the roughness height for heat compensate for the inadequacy of the stability dependence of the exchange coefficient. Unfortunately, the radiometric roughness height must then depend on the difference between the surface radiative temperature and air temperature and therefore becomes a function of the flow. The traditional similarity theory can be applied only to gradient transfer within the stability range $-5 < z/L < 1$. Therefore, the radiometric roughness height will be estimated from the datasets only after removing points outside this stability range and removing the countergradient points.

The application of the radiometric roughness height is useful in models only if the value of the radiometric roughness height can be predicted. For sparse vegetation, Kustas et al. (1989) found that $B^{-1} = (1/k)\ln(z_m/z_{hr})$ is well correlated with $\Delta\theta U$ with values ranging between 1 and 11. Brutsaert (1982), Beljaars and Holtslag (1991), and Kohsiek et al. (1993) have reported values of B^{-1} ranging from 6 to 22. Given z_m and a predictive formulation for B^{-1}, a value of z_{hr} can be estimated.

The roughness height for heat is now computed from traditional similarity theory (2) using the observed heat fluxes, the radiometric exchange coefficient computed from the data using (3), and the roughness height for momentum derived from traditional similarity and observed momentum fluxes. The variation of the roughness heights for heat and momentum between the different datasets are poorly related (Fig. 4), probably due to the different physics of each roughness height. The roughness height for momentum is related to the actual roughness of the surface and can depend on wind direction and large pressure drag associated with bluff roughness elements. In contrast, the radiometric roughness height for heat appears to be determined mainly by the dominant surface type covering the area (Beljaars and Holtslag 1991), and in the present analysis, it does not appear to depend on the roughness of the surface. The roughness height for momentum at each of the tower sites varies by several orders of magnitude. This large variation involves a small number of points and is not well correlated with wind direction or stability. Most of these points are probably related to flux-sampling problems and nonstationarity.

The present study does not attempt to justify the physics of the radiometric roughness height, but rather estimates the required variation of the radiometric roughness height for application of the bulk aerodynamic formulation with the surface radiative tempera-

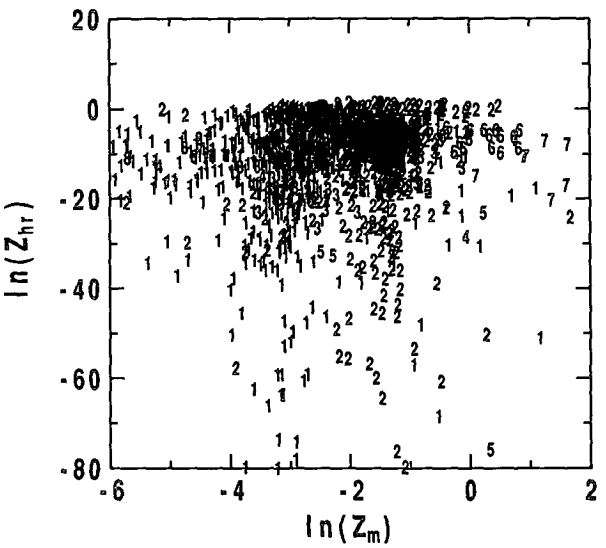

FIG. 4. Roughness height for momentum $\ln(z_m)$ versus radiometric roughness height for heat $\ln(z_{hr})$. Here 3% of the points are offscale. Both z_m and z_{hr} are in meters. See Fig. 3 for further explanation.

ture. By substituting (2) into (4), the radiometric roughness height for heat can be expressed as

$$\ln(z_{hr}) = \ln(z) + k\Delta\theta/\theta_* - \Psi_h(z/L). \quad (7)$$

The values of the stability function $\Psi_h(z/L)$ based on the Monin–Obukhov similarity theory ranges from -5 to about 3 for the valid stability range of $z/L = -5$ to $z/L = 1$. As a result, $\Psi_h(z/L)$ is much smaller than $\Delta\theta/\theta_*$ for unstable conditions when the surface radiative temperature is used to compute $\Delta\theta$. Therefore, $\Delta\theta/\theta_*$ is the dominant term on the right-hand side of (7), and the radiometric roughness height becomes closely related to variations of $\Delta\theta/\theta_*$ (Fig. 5). In other words, for gradient transfer the logarithmic term $\ln(z/z_{hr})$ in (2) must be much larger than the stability correction term Ψ_h, which in turn requires that the radiometric roughness height be extremely small for large instability. This is consistent with the stability independence of the radiometric exchange coefficient for heat (section 3).

Extremely small values of the computed radiometric roughness height result from near zero heat flux and nonzero vertical temperature difference. In these cases, small errors in the heat flux lead to enormous variations of the log of the roughness length. Therefore, extremely small values of the roughness length, corresponding to 6% of the data, have been arbitrarily omitted in Fig. 5 and the following regression analysis.

The dominance of variations of $\Delta\theta/\theta_*$ on the right-hand side of (7) suggests that the variation of the radiometric roughness height can be related to $\Delta\theta/\theta_*$ alone. In fact, the variation of the radiometric roughness height in Fig. 5 can be approximated as

$$\ln(z_{hr}) = c_1 + c_2(-\Delta\theta/\theta_*), \quad (8)$$

where $c_1 = 1.53$ and $c_2 = -0.37$. This regression relationship explains 98% of the variance of the log of the radiometric roughness height. Therefore, Monin-Obukhov similarity theory reduces to a tight relationship between the radiometric roughness height and the ratio $-\Delta\theta/\theta_*$, which could be viewed as a circular expression. Furthermore, the roughness height becomes a function of the flow itself in contrast to the classical definition of roughness heights.

The radiometric roughness height for heat encounters special observational problems in asymptotic cases. The largest values of the radiometric roughness height occurs when the measured heat flux remains significant downward ($z/L > 0$) and the measured vertical temperature difference nearly vanishes. This behavior could be related to the microscale distribution of surface radiative temperature discussed in section 3c. The values of the roughness height for heat can exceed the value of the observational height when $\Delta\theta$ becomes very small with nonzero downward heat flux, as can be shown by neglecting $-\Delta\theta/\theta_*$ on the right-hand side of (7) and noting that $\Psi(z/L)$ is negative for stable conditions.

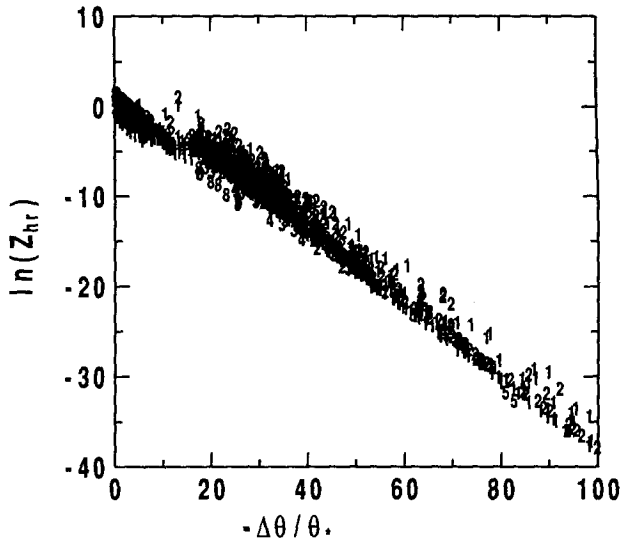

FIG. 5. Radiometric roughness height for heat $\ln(z_{hr})$ versus $-\Delta\theta/\theta_*$. Here 6% of the points are offscale. Term z_{hr} is in meters. See Fig. 3 for further explanation.

Most of the values of the radiometric roughness height are very small. These values have no direct physical meaning in that they are many orders of magnitude smaller than any actual roughness elements. Instead, the extremely small values represent a "tuning" of the roughness height to compensate for the inappropriateness of the existing stability function with use of the surface radiative temperature. The smallest values of the roughness height occur with tower observations over the irrigated cotton and vineyard.

Figures 4 and 5 indicate that for the present datasets, relating the radiometric roughness height for heat to the momentum roughness height is not the optimal approach. Apparently the success of previous relationships for B^{-1} is due to the relationship of the radiometric roughness height for heat with $(-\Delta\theta/\theta_*)$ and not due to any relationship between z_m and z_{hr}. However, categorically aborting parameterization of B^{-1} is not recommended since the generality of our results is not known and the necessary specification of z_m in modeling studies allows convenient computation of z_{hr} from B^{-1}.

5. Radiometric exchange coefficient and roughness height for moisture

The moisture flux can be estimated in terms of the bulk aerodynamic formulation based on the saturation specific humidity at the surface radiative temperature

$$\overline{w'q'} = C_{vr}U\Delta q, \quad (9)$$

where

$$\Delta q = q_s(T_{sfc}) - q_a.$$

Here C_{vr} is the radiometric exchange coefficient for moisture, $q_s(T_{sfc})$ is the saturation specific humidity at the surface radiative temperature T_{sfc}, and q_a is the specific humidity measured from the tower or aircraft. Since (9) relates the moisture flux to the surface saturation humidity, C_{vr} decreases with increasing soil moisture deficit and stomatal control. A more traditional definition of C_{vr} would absorb the dependence on soil moisture by attempting to estimate an actual specific humidity at the surface.

Analogous to the radiometric exchange coefficient for heat (5), the radiometric exchange coefficient for the moisture flux is closely approximated by the following relationship:

$$C_{vr} = a_v(-q_*/\Delta q), \qquad (10)$$

where q_* is defined as $-\overline{w'q'}/u_*$. To evaluate (10), the largest 1% of the values of the exchange coefficient were excluded because of suspected measurement errors (section 3b). The corresponding data are plotted in Fig. 6. The nonzero constant resulting from the regression analysis was extremely small and was neglected. The best-fit value of a_v is 0.095. The resulting relationship explains 84% of the variance of C_{vr}.

Because of the use of the saturation specific humidity with surface radiative temperature, Δq is generally positive for these data even when T_{sfc} is smaller than T_a. Since the moisture flux is generally upward for this data, the moisture flux is usually gradient and $-\Delta q/q_*$ is usually positive (Fig. 7). Nonetheless, a few cases of countergradient moisture flux occur in the tower data over the irrigated cropland mainly with negative values of Δq with weak upward moisture flux (Fig. 7). These countergradient cases must be removed

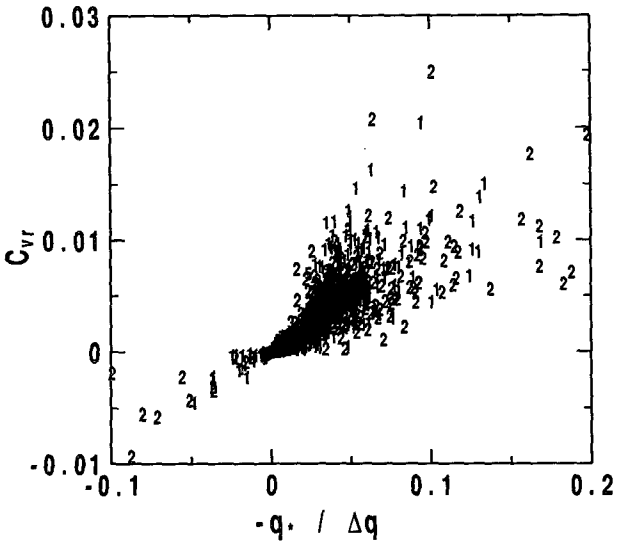

FIG. 6. Radiometric exchange coefficient for moisture as a function of $-q_*/\Delta q$. Here 1% of the points are offscale. See Fig. 3 for further explanation.

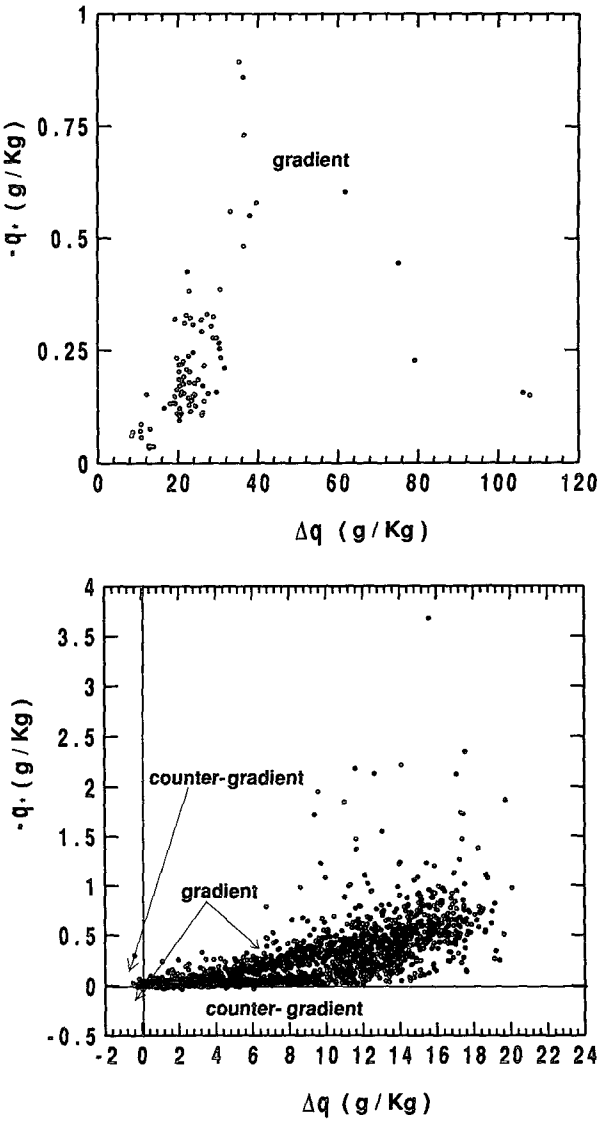

FIG. 7. (a) The aircraft data and (b) the tower data in phase space based on $-q_*$ and Δq.

in order to use traditional similarity theory. Extremely small values of the roughness length, equal to 7% of the data, have also been removed for reasons discussed in section 4.

Similar to the radiometric roughness height for heat, the radiometric roughness height for moisture z_{vr} can then be expressed as (Fig. 8)

$$\ln(z_{vr}) = e_1 + e_2(-\Delta q/q_*). \qquad (11)$$

For the present datasets, e_1 and e_2 are found to be 1.54 and -0.39, respectively. The resulting relationship explains nearly 100% of the variance of $\ln(z_{vr})$. The high percentage of the variance explained in this relationship is partly due to the exponential increase of saturation specific humidity with surface radiative temperature.

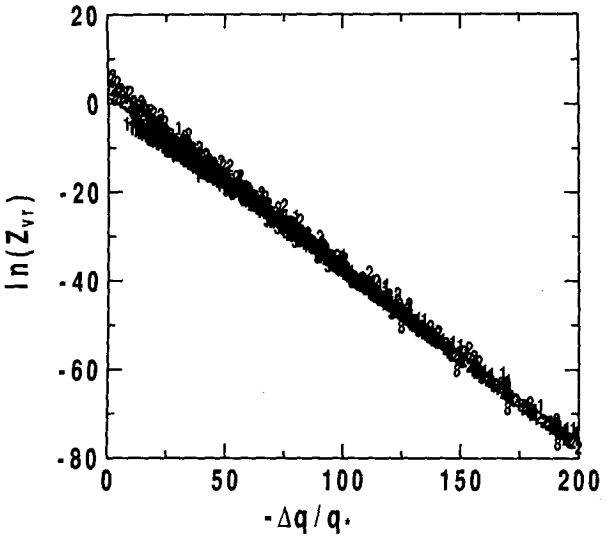

FIG. 8. Radiometric roughness height for moisture as a function of $-\Delta q/q_*$. Here 7% of the points are offscale. Term z_{vr} is in meters. See Fig. 3 for further explanation.

Analogous to the role of $\Delta\theta$ in (7), the large values of Δq plays a dominant role compared to $\Psi_v(z/L)$ in determination of $\ln(z_{vr})$.

Again, the radiometric roughness height for moisture is an adjustable parameter that allows the traditional similarity theory to predict the correct moisture flux with use of surface radiative temperature. This variable roughness height depends on the flow as well as soil moisture and has no obvious relationship to the surface roughness elements. The largest values of the radiometric exchange coefficient and roughness height for moisture correspond to nonzero flux in presence of the vanishing Δq, while the near zero values of the radiometric exchange coefficient and roughness height correspond to vanishing moisture flux in the presence of nonvanishing Δq. These extreme values occur with the tower data.

6. Other stability functions

Section 4 showed that the radiometric roughness height for heat is dominated by the variation of $(-\theta_*/\Delta\theta)$ when the traditional Monin–Obukhov similarity theory is used. In this section, additional stability functions are examined. For the range of values of the roughness height for momentum typically reported in the literature, the traditional similarity theory predicts very small drag coefficients for very stable conditions where L becomes smaller than the observation height.

a. Louis formula

As a simplifying approximation to the Paulson stability dependence, Louis (1979) and Louis et al. (1981) formulated an exchange coefficient that depends on the bulk Richardson number. The Louis formula is explicit, whereas traditional similarity theory based on the Paulson formula is implicit in that the exchange coefficient is a function of the Obukhov length, which depends on the fluxes. Therefore, the Louis formulation is widely used in numerical models. For unstable conditions (large negative z/L) and specified roughness heights for heat and momentum, the exchange coefficient estimated from Louis can become significantly larger than those predicted by the Paulson formula shown in Fig. 9. This error is large whenever the roughness height for heat is very small compared to the roughness height for momentum, which must occur with use of the radiative temperature for large $-\Delta\theta/\theta_*$ (Fig. 5). Analogous errors influence the prediction of moisture fluxes.

As an additional comparison, the radiometric roughness height for heat is computed using the Louis formula and roughness height for momentum. To isolate differences in the roughness height for heat, the roughness height for momentum is computed from the observed fluxes and the Paulson stability function. For stable conditions, the roughness heights for heat computed from the two formulas are similar (upper left part of Fig. 10). This agreement was also evident in Fig. 9 for stable conditions where the roughness height for heat is specified to be small. For unstable conditions, the roughness height for heat predicted by the Louis formulation is much smaller than the value using the Paulson stability function. This is due to the inaccuracy of the Louis approximation for unstable conditions where the roughness height for heat is much smaller than that for momentum, as also shown in Fig. 9.

b. Brutsaert stability function

Sugita and Brutsaert (1990) show that the radiometric roughness height corresponding to the Businger-Dyer stability function decreases with solar elevation angle. Since higher-elevation angle implies greater $\Delta\theta$, these results are consistent with the results of this study as in (8).

Brutsaert (1992) developed a new stability similarity function for unstable conditions based on a combination of the proposal of Kader and Yaglom (1990) and the data analysis of Högström (1988). This stability function is written as

$$\Psi_h(z/L) = 1.20 \ln\left[\frac{0.33 + (-z/L)^{0.78}}{0.33 + (-z_{hr}/L)^{0.78}}\right]. \quad (12)$$

The radiometric roughness height based on the Brutsaert stability function, which is applicable for use of surface radiative temperature, is much smaller than that based on the Paulson stability function (Fig. 11).

7. Conclusions

The bulk aerodynamic formulas for heat and moisture using the surface radiative temperature have been

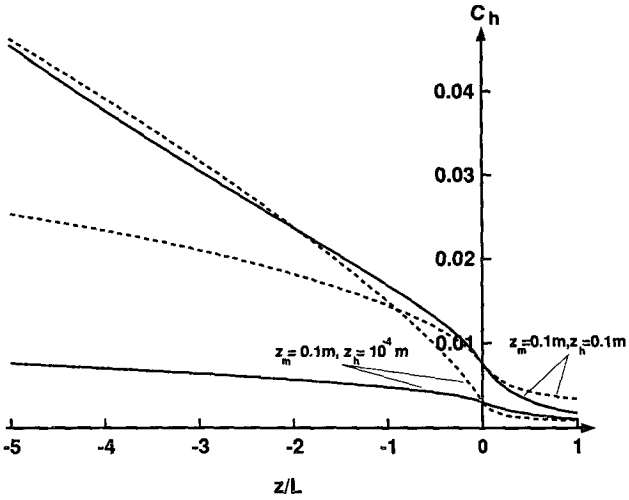

FIG. 9. Comparison between the exchange coefficients derived from the Paulson (solid) and the Louis formula (dashed) for $z = 10$ m. Case 1: $z_m = 0.1$ m and $z_h = 0.1$ m. Case 2: $z_m = 0.1$ m and $z_h = 10^{-4}$ m.

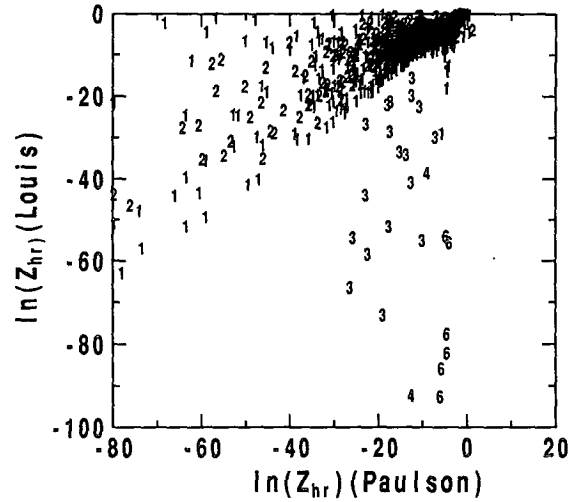

FIG. 10. Comparison between the radiometric roughness heights for heat derived from the Paulson and Louis formulas. Here 15% of the points are offscale. Both roughness heights are in meters. See Fig. 3 for further explanation.

evaluated using aircraft and tower measurements in order to study the behavior of the corresponding exchange coefficients, here referred to as the *radiometric exchange coefficients.* This analysis has been used to evaluate the common practice of predicting the surface heat flux from Monin–Obukhov similarity theory and the surface radiative temperature or temperature from the surface energy budget. The traditional stability dependence for Monin–Obukhov similarity theory does not apply when the surface radiative temperature is used instead of aerodynamic temperature at roughness height. The large difference between the surface radiative temperature and air temperature for unstable conditions requires that the radiometric exchange coefficient is significantly smaller than the one predicted from traditional similarity theory. More specifically, the stability term in (7) becomes negligible compared to the term containing $\Delta\theta/\theta_*$, leading to a more constrained relationship between the roughness height for heat and $\Delta\theta/\theta_*$.

As an additional consequence of use of the surface radiation temperature, the variation of the radiometric exchange coefficient is almost completely explained by the variation of $\theta_*/\Delta\theta$ for the full range of stability conditions and is independent of the roughness of the surface. This tight relationship between the radiometric exchange coefficient and $\theta_*/\Delta\theta$ results from the fact that the variations of the drag coefficient are small compared to variations of $\theta_*/\Delta\theta$ (section 3). This relationship could be viewed as a circular one with dubious predictive value, but it nonetheless accurately describes a simplified internal relationship for the radiometric exchange coefficient for a wide variety of situations.

The traditional stability function for Monin–Obukhov similarity theory cannot be adjusted to accomodate use of the surface radiative temperature. "Tuning" the roughness height for heat so that existing Monin–Obukhov similarity theory correctly predicts the surface fluxes leads to unphysically small values for unstable conditions because of the large temperature difference between surface radiative temperature and air temperature. Furthermore, this radiometric roughness height depends on the flow and is poorly related to the roughness height for momentum. In this sense, the roughness height for heat is a poorly defined parameter for the common use with the surface radiation temperature. Analogous problems result with the

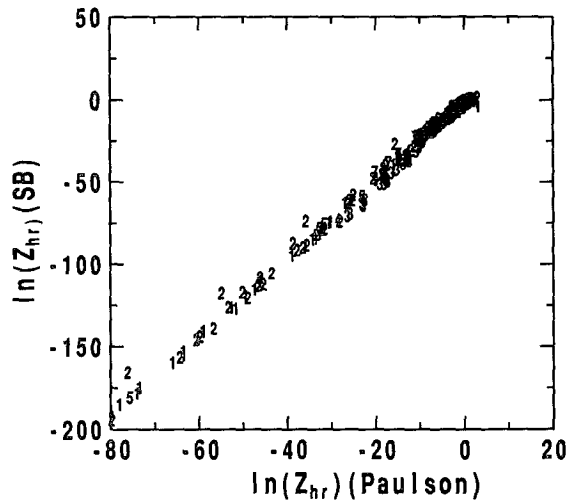

FIG. 11. Comparison between the radiometric roughness heights for heat derived from the Paulson and Brutsaert stability functions. Here 3% of the points are offscale. Both roughness heights are in meters. See Fig. 3 for further explanation.

prediction of the moisture flux based on the saturation vapor pressure computed from the surface radiation temperature (section 5).

The excellent approximation of the Louis formula to the traditional similarity theory with the Paulson stability function breaks down if the roughness height for heat is very small as occurs with use of the surface radiative temperature for unstable conditions (section 6). As a result, the roughness height for heat derived from the Louis approximation is smaller than that derived from the Paulson formula. The radiometric roughness height derived from the Brutsaert stability function is smaller than, but closely related to, that derived from the Paulson formula.

This study also suggests that using a single radiometer for measurement of the surface radiative temperature may be inadequate for partially vegetated surfaces. For example, countergradient heat fluxes are observed over irrigated crops apparently due to domination of the heat flux by the unshaded bare soil between the rows, while the radiation footprint is dominated by the cooler transpiring vegetation. Measurements of the distribution of the surface radiative temperature within the footprint of the heat flux measurement are required before a more definitive similarity theory for the radiometric exchange coefficient can be constructed.

Acknowledgments. The comments of the reviewers and Bill Kustas are greatly appreciated. This material is based upon work supported by Grant DAAH04-93-G-0019 from the Army Research Office and Grant ATM-9310576 from the Physical Meteorology Program of the National Science Foundation. The graphics assistance of Michael Ek and programming assistance of Dean Vickers are greatly appreciated. The authors acknowledge Ian MacPherson and Ray Desjardin for providing the CODE aircraft data, Steve Oncley for providing ASTER data, Tom Lyons and Xinmei Huang for providing the buFex data, G. den Hartog for providing the tower data at the grape site, and Roland Stull for providing the BLX 83 data.

REFERENCES

Beljaars, A. C., and A. A. M. Holtslag, 1991: Flux parameterization over land surfaces for atmospheric models. *J. Appl. Meteor.*, **30,** 327–341.

Brutsaert, W. H., 1982: *Evaporation into the Atmosphere—Theory, History, and Applications.* Reidel, 299 pp.

——, 1992: Stability correction functions for the mean wind speed and temperature in the unstable surface layer. *Geophys. Res. Lett.*, **19,** 469–472.

——, and M. Sugita, 1992: Regional surface fluxes from satellite-derived surface temperatures (AVHRR) and radiosonde profiles. *Bound.-Layer Meteor.*, **58,** 355–366.

Choudhury, B. J., R. J. Reginato, and S. B. Idso, 1986: An analysis of infrared temperature observation of wheat and calculation of latent heat flux. *Agric. For. Meteor.*, **37,** 75–88.

Delany, A., S. Semmer, T. Horst, S. Oncley, C. Martin, and W. Massman, 1993: The ASTER development at the cotton site during the California Ozone Depositional Experiment 91 of the San Joaquin Valley air quality study. National Center for Atmospheric Research, Boulder, CO, 61 pp.

den Hartog, G., R. E. Mickle, H. H. Neumann, J. Arnold, J. Deary, and A. Beavan, 1992: Final documentation report on vineyard measurements for the San Joaquin Valley Air Pollution Study Agency, Contract 91-2. The Air Quality Processes Research Division Atmospheric Environment Service, Downsview, Ontario, 101 pp.

Garratt, J. R., and R. J. Francey, 1978: Bulk characteristics of heat transfer in the unstable, baroclinic atmosphere boundary layer. *Bound.-Layer Meteor.*, **15,** 399–421.

Hall, F. G., K. F. Huemmrich, S. J. Goetz, P. J. Sellers, and J. E. Nickeson, 1992: Satellite remote sensing of surface energy balance: Success, failures, and unresolved issues in FIFE. *J. Geophys. Res.*, **97,** 19 061–19 089.

Hatfield, J. L., R. J. Reginato, and S. B. Idso, 1984: Evaluation of canopy temperature-evapotranspiration models over various crops. *Agric. For. Meteor.*, **32,** 41–53.

Högström, U., 1988: Non-dimensional wind and temperature profiles in the atmospheric surface layer: A re-evaluation. *Bound.-Layer Meteor.*, **42,** 55–78.

Kader, B. A., and A. M. Yaglom, 1990: Mean fields and fluctuation moments in unstably stratified turbulent boundary layers. *J. Fluid. Mech.*, **212,** 637–662.

Kohsiek, W., H. A. R. De Bruin, H. The, and B. Van Den Hurk, 1993: Estimation of the sensible heat flux of a semi-arid area using surface radiative temperature measurements. *Bound.-Layer Meteor.*, **63,** 213–230.

Kustas, W. P., B. J. Choudhury, M. S. Moran, R. J. Reginato, R. D. Jackson, L. W. Gay, and H. L. Weaver, 1989: Determination of sensible heat flux over sparse canopy using thermal infrared data. *Agric. For. Meteor.*, **44,** 197–216.

Lhomme, J. P., N. Katerji, A. Perrier, and J. M. Bertolini, 1988: Radiative surface temperature and convective flux calculation over crop canopies. *Bound.-Layer Meteor.*, **43,** 383–392.

Louis, J.-F., 1979: A parametric model of vertical eddy fluxes in the atmosphere. *Bound.-Layer Meteor.*, **17,** 187–202.

——, M. Tiedke, and J. F. Geleyn, 1981: A short history of the operational PBL parameterization at ECMWF. *Workshop on Planetary Boundary Layer Parameterization,* ECMWF, 59–79.

Lyons, T. J., P. Schwerdtfeger, J. M. Hacker, I. J. Foster, R. C. G. Smith, and Huang Xinmei, 1993: Land-atmosphere interaction in a semiarid region: The Bunny Fence Experiment. *Bull. Amer. Meteor. Soc.*, **74,** 1327–1324.

MacPherson, J. I., 1992: NRC Twin Otter operations in the 1991 California Ozone Deposition Experiment. Rep. LTR-FR-118. Flight Research Laboratory, National Research Council, Ottawa, 41 pp.

Mahrt, L., 1991: Eddy asymmetry in the sheared heated boundary layer. *J. Atmos. Sci.*, **48,** 472–492.

——, and M. Ek, 1993: Spatial variability of turbulent fluxes and roughness lengths in HAPEX-MOBILHY. *Bound.-Layer Meteor.*, **65,** 381–400.

Otterman, J., T. W. Brakke, and J. Susskand, 1992: A model for inferring canopy and underlying soil temperatures from multi-directional measurements. *Bound.-Layer Meteor.*, **61,** 81–98.

Paulson, C. A., 1970: The mathematical representation of wind speed and temperature profiles in the unstable atmospheric surface layer. *J. Appl. Meteor.*, **9,** 857–861.

Pederson, J. R., and collaborators, 1994: California ozone deposition experiment, methods, results and opportunities. *Atmos. Environ.*

Stull, R. B., 1994: A convective transport theory for surface fluxes. *J. Atmos. Sci.*, **51,** 3–22.

Sugita, M., and W. Brutsaert, 1990: Regional surface fluxes from remotely sensed skin temperature and lower boundary layer measurements. *Water Resour. Res.*, **26,** 2937–2944.

Sun, J., and L. Mahrt, 1994: Spatial distribution of surface fluxes estimated from remotely sensed variables. *J. Appl. Meteor.*, **33,** 1341–1353.

Zilitinkevich, S. S., 1970: *Dynamics of the Atmospheric Boundary Layer.* Leningrad Gidrometeor, 291 pp.